SCIENCE CHINA
Information Sciences

April 2019, Vol. 62 040301:1–040301:26
https://doi.org/10.1007/s11432-018-9811-0

• REVIEW •
Special Focus on High-Resolution Radar

Advanced technology of high-resolution radar: target detection, tracking, imaging, and recognition

Teng LONG, Zhennan LIANG & Quanhua LIU*

Radar Research Laboratory, School of Information and Electronics, Beijing Institute of Technology, Beijing 100081*, China*

Received 12 January 2019/Revised 19 February 2019/Accepted 4 March 2019/Published online 11 March 2019

Abstract In recent years, the performances of radar resolution, coverage, and detection accuracy have been significantly improved through the use of ultra-wideband, synthetic aperture and digital signal processing technologies. High-resolution radars (HRRs) utilize wideband signals and synthetic apertures to enhance the range and angular resolutions of tracking, respectively. They also generate one-, two-, and even three-dimensional high-resolution images containing the feature information of targets, from which the targets can be precisely classified and identified. Advanced signal processing algorithms in HRRs obtain important information such as range-Doppler imaging, phase-derived ranging, and micro-motion features. However, the advantages and applications of HRRs are restricted by factors such as the reduced signal-to-noise ratio (SNR) of multi-scatter point targets, decreased tracking accuracy of multi-scatter point targets, high demands of motion compensation, and low sensitivity of the target attitude. Focusing on these problems, this paper systematically introduces the novel technologies of HRRs and discusses the issues and solutions relevant to detection, tracking, imaging, and recognition. Finally, it reviews the latest progress and representative results of HRR-based research, and suggests the future development of HRRs.

Keywords high-resolution radar, integrated detection and tracking, multiple target tracking, phase-derived velocity, inverse synthetic aperture radar(ISAR), hierarchical classification, convolution neural network

Citation Long T, Liang Z N, Liu Q H. Advanced technology of high-resolution radar: target detection, tracking, imaging, and recognition. Sci China Inf Sci, 2019, 62(4): 040301, https://doi.org/10.1007/s11432-018-9811-0

1 Introduction

During World War II, radar was invented as a remote sensor with all-weather, all-time capability. Over the past 80 years or thereabouts, radar has provided humans with clairvoyance and clairaudience and has been widely applied in both national defense and civilian activities [1–17]. The examples include surveillance, reconnaissance, navigation, fire control, and traffic control.

The first practical radar system, developed by Britain in the 1930s, detected targets using a single pulse. At the end of World War II, the moving target indication radar was invented, which could distinguish moving targets from clutter by the phase changes of the echoes in adjacent transmitter–receiver periods. In the 1950s, the United States developed the pulse-Doppler (PD) radar, which obtained the Doppler frequency from the phase changes of the target echoes in multiple successive pulse cycles. Therefore, the PD radar could suppress clutter more effectively and measure the target velocity with higher accuracy than the previous radars. In the mid-1950s, the United States also developed the phased-array radar, in which a beam of radio waves generated by a computer-controlled array of antennas could be electronically steered in different directions. Unlike the mechanical scanning radar, the phased-array radar searches,

* Corresponding author (email: liuquanhua@bit.edu.cn)

detects, and tracks multiple batches of targets in different directions simultaneously, with quick switching of the beam direction. Its benefits include multi-functionality, agility, change celerity, high data rate, strong anti-interference ability, and high reliability [1–5].

Radar waveforms have always played an important role in radar development [6]. In 1943, North [7] pointed out the importance of a matched filter (the basis of radar signal processing) in detecting the targets among echo signals with known transmitted waveforms. In 1953, Woodward [8] evaluated the range and Doppler resolution of transmitting waveforms by using an ambiguity function, laying the foundation of radar waveform design. Dicke [9] proposed the use of linear frequency modulation signals in matched filtering, where a signal with a time-bandwidth product larger than one effectively solved the contradiction between the range resolution and signal energy. Linear frequency modulation has replaced the early unmodulated rectangular waveform as the most commonly utilized type of radar signal.

Narrowband signals are widely used in low-resolution radars (LRRs) because they can be easily generated and processed. Accordingly, the echo data are relatively low-volume, and can be easily realized in engineering activities. In general, LRRs work well for simple tasks such as detection and ranging. However, the development of electronic devices has increased the demand for advanced functions such as imaging and target recognition. Owing to their low-range resolution, LRRs obscure the fine structural information of complex targets, and can only approximately estimate the motion parameters. They also have weak anti-interference and anti-clutter ability [10]. Moreover, a target with multiple scattering centers causes an angular glint under narrowband conditions [14], and multipath echoes and the direct wave distance cannot be resolved at small elevation angles [15]. These limitations significantly reduce the tracking performance of LRRs. In addition, narrowband signals contain limited target-feature information, reducing the effectiveness of classifying and identifying the targets [11–14]. Therefore, LRRs cannot meet the requirements of target recognition.

Meanwhile, radar targets and the detection environment have become increasingly challenging [16–18]. Space surveillance is challenged by the proliferation of fast, highly mobile, dense, and weakly detectable targets (spacecraft and space debris, warheads, and decoys from ballistic missile defense systems and dense unmanned aerial vehicle colonies), which inhabit space, the atmosphere, and the ground. In addition, the rapid development of electronic countermeasures [19, 20] causes strong active jamming, which may impact effective target detection. Effectively distinguishing the target among the jammed signals has become the core of improving radar performance.

To meet the increasingly complex requirements of target recognition, modern research has focused on high-resolution radars (HRRs) with high range resolution and high angle resolution [11–14, 21, 22]. The unique advantages of HRRs in detection, tracking, imaging, and parameter measurement have improved the performance of target recognition. First, the increased radar-signal bandwidth of an HRR reduces the range resolution to below the target size. The target is distributed among multiple range-resolution units, thereby suppressing its radar cross-section (RCS) fluctuations and improving the detection performance. The superior detection and tracking performances of HRRs are especially evident under clutter and jamming conditions. Second, the synthetic aperture radar (SAR) and inverse synthetic aperture radar (ISAR) can effectively compensate the platform or uncoordinated movements of the target during the tracking period, obtaining two-dimensional high-resolution images [23–29]. Third, the measurement accuracy of HRRs can be improved by advanced signal processing algorithms, enabling high-precision phase-derived velocity measurement (PDVM) [30, 31] and micro-motion feature extraction [32–35].

In general, accurate target recognition is benefitted by abundant target information (such as the micro-characteristics of the target and echo amplitudes of the scattering points), high measurement accuracy, and a high tracking-data rate. However, the advantages and applicability of HRRs are restricted by factors such as low signal-to-noise ratio (SNR), several false alarms (which decreases the tracking accuracy of multi-scatter point targets), high demands of motion compensation, and sensitivity of the target attitude [11–14]. These limitations cause problems in detection, tracking, imaging, and recognition by HRRs, as outlined below:

(1) In HRR detection, the echo energy of the target is dispersed into multiple range units, which decreases the SNR. In addition, the range resolution unit of HRRs is very small. Therefore, as the target

moves between adjacent pulses, the target-echo envelope often moves across the range unit, affecting the long-term integration of the target echo. Both problems reduce the target detection performance and shorten the operating range of the HRR.

(2) In HRR tracking, the enlarged signal bandwidth decreases the size of the radar range resolution unit, increasing the false-alarm density. Together with the decreased SNR of detection, the increased false-alarm density raises the performance demands on the data association module and track filter module.

(3) In HRR imaging, the enlarged imaging range reduces the SNR. To correct this problem, radar imaging research has focused on the motion compensation technique and imaging methods that cope with low SNR data. ISAR motion compensation and imaging algorithms are required under discontinuous or sparse conditions. Multi-target ISAR imaging technique is gaining relevance in today's increasingly complex imaging environments.

(4) Finally, the fairness of the data in classifying and recognizing targets in one-dimensional high-resolution images is influenced by three factors, namely target-aspect sensitivity, translation sensitivity, and amplitude sensitivity. The training samples are usually ideal data obtained with a sufficiently high SNR, whereas the test data are collected in variable environments with differing SNRs. When the signal energy is low, the one-dimensional image is affected by environmental noise, clutter, and other interferences, which seriously reduce the recognition performance of the HRR.

Focusing on these problems, this paper systematically introduces the novel technologies of an HRR and discusses the relevant issues and solutions in detection, tracking, imaging, and recognition by the HRR. Finally, it presents the latest progress and representative results of HRR-based research, and the prospective development of HRRs.

2 Development of HRR

The development of HRR originated from the demands of space-target observations [14,21]. Space targets include man-made satellites (such as space stations and spacecraft), space debris, ballistic missiles, and other objects launched into the atmosphere. As the space target is far away, the detection range of ground-based instruments must be as long as possible, perhaps up to 5000 km. The required detection range of space-target radar generally ranges from 1000 to 5000 km. Meanwhile, to image satellites and space debris and to distinguish multiple targets, the space-target radar requires a high range resolution, which is usually achieved by enlarging the signal bandwidth. Finally, the space-target radar should achieve rapid beam scanning and beam forming, as well as multi-target detection and tracking.

Obviously, space-target detection would improve the implementations of national air defense, anti-missile actions, strategic early warnings, and command automation of sovereign countries. For this purpose, it is necessary to innovate the radar system, signal waveform, and signal processing. These innovations have largely promoted the development of HRRs. How to improve radar detection, parameter estimation, continuous estimation, imaging identification, and recognition comprise the technical challenges of "integration of HHRs detection and tracking".

HRRs are mainly applied in the military field. To effectively resolve and identify the warheads and decoys in ballistic missile defense systems, the Lincoln Laboratory of the United States began researching wideband radars in the 1960s. This study culminated in the world's first wideband radar ALCOR [36] in 1970, which utilized waveforms with a bandwidth of 512 MHz in reentry tracking. In the 1990s, the wideband phased-array ground-based radar (GBR) working in the X-band was an important component of national missile defense and the U.S. terminal high altitude area defense (THAAD) system. GBR performs a series of tasks such as target detection, tracking, and threat classification. Antimissile tests using GBR-P, a GBR prototype developed by Raytheon Company (headquartered in Waltham, Massachusetts, USA), were successfully carried out in September 2000[1)2)]. The sea-based X-band radar operates over a

1) http://www.fas.org/spp/starwars/program/news00/bmd-001012.html.
2) http://defensenewsstand.com/Inside-Missile-Defense/Inside-Missile-Defense-10/04/2000/menu-id-291.html.

bandwidth of 1 GHz [37]. To improve the operational capability of the ballistic missile defense system in detecting outer space movements, the United States developed transportable FBX-T radar, which enlarges the signal bandwidth of THAAD-GBR from 500 MHz to 1 GHz. The tracking and imaging radar (TIRA) system developed in Germany works in both the L- and Ku-bands. The Ku-band is used for wideband imaging with an initial bandwidth of 800 MHz. After continuous upgrading, the Ku bandwidth of TIRA has reached 2.1 GHz [38].

3 Range-spread target detection technology

When the range resolution is lower than the target size, the original ideal point target is spatially resolved into several scattering cells, thereby becoming a range-spread target. The resulting spatial-scattering density provides abundant information on the target (such as its length, structure, and attitude), and decreases the fluctuations in the received signals. These advantages improve the detection performance of the radar, especially in cluttered environments [39].

However, spatially distributed target detection is disadvantaged by low SNR. High-range resolution disperses the echo power into multiple range cells, but in a certain noise-temperature situation, high-range resolution means a larger signal bandwidth, and consequently, a larger noise power at the receiver. Both factors decrease the detection performance and reduce the operating range of HRRs. As the traditional matched filter cannot completely integrate the echo energy, the typical detection method is no longer applicable, and must be replaced by algorithms that detect range-spread targets.

Over the past few decades, many studies have integrated the energies of the scattering cells and extracted the characteristics of the target signature [39–55]. Some outcomes of these studies are elaborated below.

First, the classical point-target detector was modified for range-spread targets by the energy integration detector and the M out of N (M/N) detector. The typical scattering density dependent generalized likelihood ratio test (SDD-GLRT) detector [39], which consists of a nonlinear map followed by an integrator along the range cells, detects a range-spread target among white Gaussian noise. If the scattering density parameter is known, the performance of SDD-GLRT improves. However, the efficiency of SDD-GLRT solutions is decreased by the exponential and logarithmic operations. The M/N detector is a typical double-threshold detector of spatially distributed targets. Owing to its efficient structure, this detector can be easily realized in engineering and has been widely applied. Therefore, it has attracted much interest and has been often modified to improve its robustness and efficiency [40, 41, 55].

Second is the adaptive detector, which utilizes multiple high-resolution range profiles (HRRPs) collected from consecutive pulses or antenna subarrays to cope with cluttered backgrounds [42–49]. The authors of [42] introduced a GLRT-based adaptive detector of range-spread targets in a partially uniform cluttered environment. The authors of [45] considered range-spread target detection in spherically invariant random-vector clutter, and developed different detectors with a constant false alarm rate by exploiting the order-statistics theory. In [46], a generalized matched subspace detector and a general adaptive subspace detector in the frequency domain were developed for range-spread targets with range-walking in a partially homogeneous clutter. The authors of [49] developed adaptive decision schemes that reveal extended targets along with structured unwanted components in random interference (clutter and thermal noise).

Third, to cope with the abundant information of the target signature, researchers have proposed range-spread target detectors using multiple HRRPs in various environments. These systems detect range-spread aircraft with maneuvering flights [50–54]. The detector proposed in [50] is based on the cross time-frequency distribution features of two adjacently received signals, whereas that in [51] exploits the waveform entropy of the arithmetic average of multiple successive HRRPs. The detector in [52] uses a two-dimensional nonlinear shrinkage map related to the local statistics of a range-pulse image. The authors of [53] proposed a heuristic detector that exploits the characteristics of target HRRPs extracted from real target radar data. A range-spread target detector based on the time–frequency decomposition

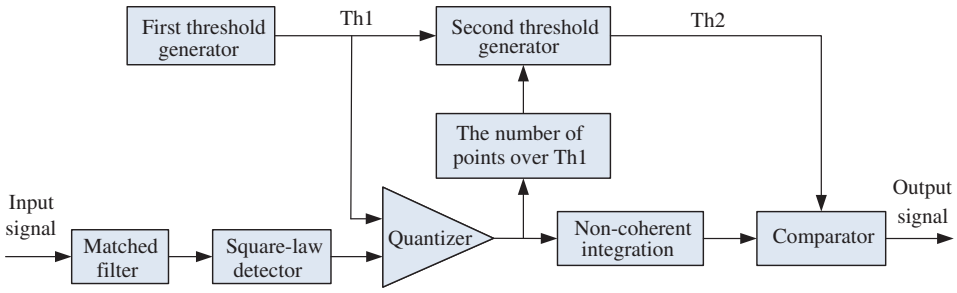

Figure 1 (Color online) Flowchart of GLRT-DT detector.

Table 1 Scattering center of target

Model number	Name	Scattering energy distribution
Model 1	Sparse uniform distribution	The target is composed of 5 scatterers, each containing 20% of the target energy.
Model 2	Sparse nonuniform distribution	The target is composed of 1 strong scatterer, 1 weak scatterer, and 3 weaker scatterers containing 70%, 20%, and 3.33% (each) of the target energy, respectively.
Model 3	Dense uniform distribution	The target is composed of 128 weak scatterers, each containing 0.78% of the target energy.
Model 4	Dense nonuniform distribution	The target is composed of 2 strong scatterers and 126 weak scatterers, each containing 20% and 0.48% of the target energy, respectively.

of two adjacent mixer outputs using the cross S-method was devised in [54].

Although some detectors of range-spread targets perform well, they are very time consuming and cannot be easily realized in engineering practice. We have extended the M/N detector to form the generalized likelihood ratio test double threshold (GLRT-DT) [55]. To improve the robustness of the detector and avoid energy loss, we added a non-quantified accumulator to the M/N detector and adjusted the detection procedure accordingly. GLRT-DT performs well even when the number of scatterers and the target location are missing. The detector is robust and delivers high detection performance. The proposed detector is schematized in Figure 1.

The detection performances of GLRT-DT have been compared with those of the integrator detector, SDD-GLRT detector, and M/N detector in Monte Carlo simulations. The scattering center of the target can encounter four situations, as shown in Table 1.

Figure 2 shows the detection performances of the integral detector, M/N detector, SDD-GLRT detector, and GLRT-DT detector under the above parameters. As shown in the figure, the proposed detector significantly outperformed the integrator detector and M/N detector. Its performance even surpassed that of the SDD-GLRT detector in a sparse scattering environment, and approached that of the SDD-GLRT detector in a dense scattering environment. Therefore, the proposed detector robustly operates in both sparse and dense scattering environments.

4 High precision phase-derived velocity measurement technology

With the rapid development of radar technology, the application demands of high-precision ranging and target velocity measurements have increased in various fields. For example, micro-motion measurements [33, 34, 56] have always been active topics in target detection and recognition. However, owing to their small amplitudes and imprecise motion compensation, micro-motions are difficult to characterize. This bottleneck is most effectively broken through by improving the accuracy of the range and velocity measurements [34, 57].

Theoretically, the precisions of the radar range and velocity measurements in conventional radar systems can be improved by increasing the signal bandwidth and integration time, respectively. However,

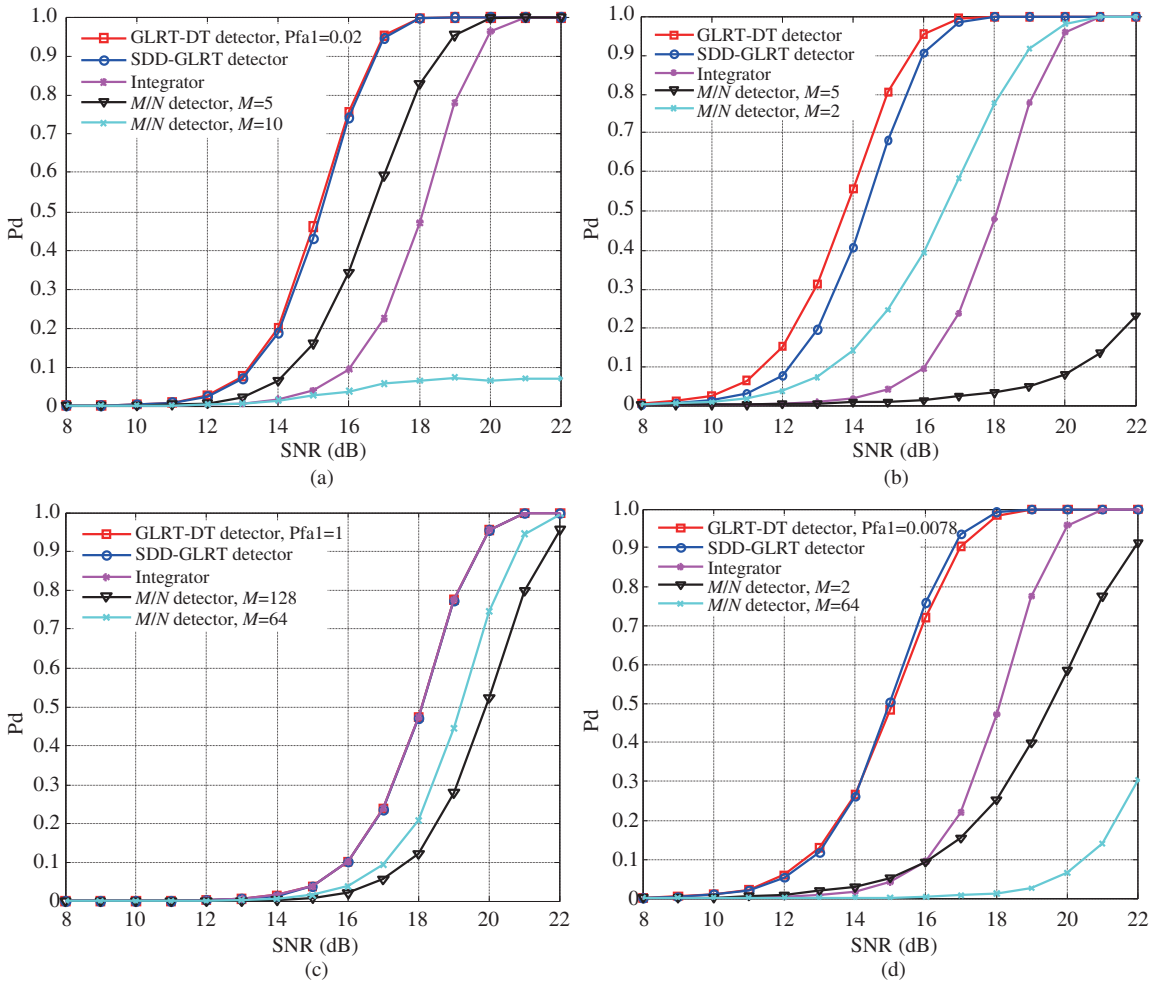

Figure 2 (Color online) Performance comparison of four detectors (integral, M/N, SDD-GLRT, and GLRT-DT). (a) Model 1: sparse uniform distribution; (b) model 2: sparse nonuniform distribution; (c) model 3: dense uniform distribution; (d) model 4: dense nonuniform distribution.

increasing the signal bandwidth reduces the range resolution of the cells, whereas increasing the integration time increases the range migration. Therefore, the range migration of a high-sped target within the integration time exceeds the range resolution of the cell. Balancing large-signal bandwidths and long-time integration is usually a difficult task.

Range and velocity measurement methods utilizing phase information have been developed since the 1970s. In the 2000s, Raytheon Company patented two methods of phase-derived range measurement (PDRM) [30, 31]. The PDRM technique extends the measurement of the target motion from macro to micro, providing more effective characteristic reference information for target recognition.

Inspired by the PDRM concept, we proposed PDVM, which measures the target velocity from the range rate of the target echoes between two adjacent frames [58]. Figure 3 shows the implementation of the high-precision phase-derived range and velocity measurements. Because the range measurement represents the range increment between two adjacent frames, the velocity of the target can be measured at high precision by dividing the range increment by the time interval between the adjacent frames. Meanwhile, the high-precision PDRM of the target can be derived by summing the range increments of two adjacent frames. The range-increment measurements can be filtered after solving the ambiguity, further improving the accuracy of the range and velocity measurements.

The measurement accuracy of the range increment between adjacent frames was simulated under different SNR conditions. The simulated envelope ranging measurement (EVM) and accuracies of the PDRM are shown in Figures 4 and 5, respectively. In the SNR range 16–35 dB, the root mean squared

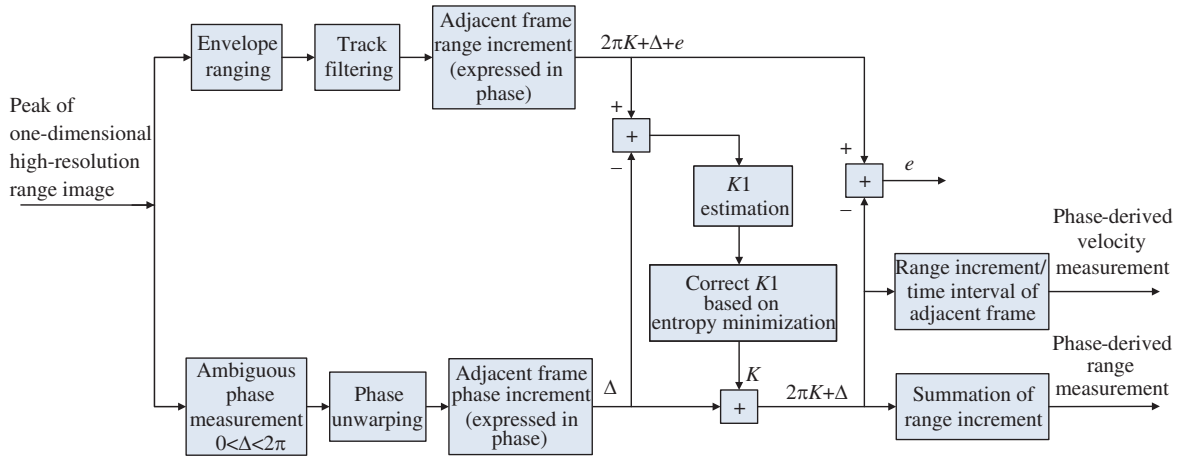

Figure 3 (Color online) Implementation of high-precision phase-derived range and velocity measurements.

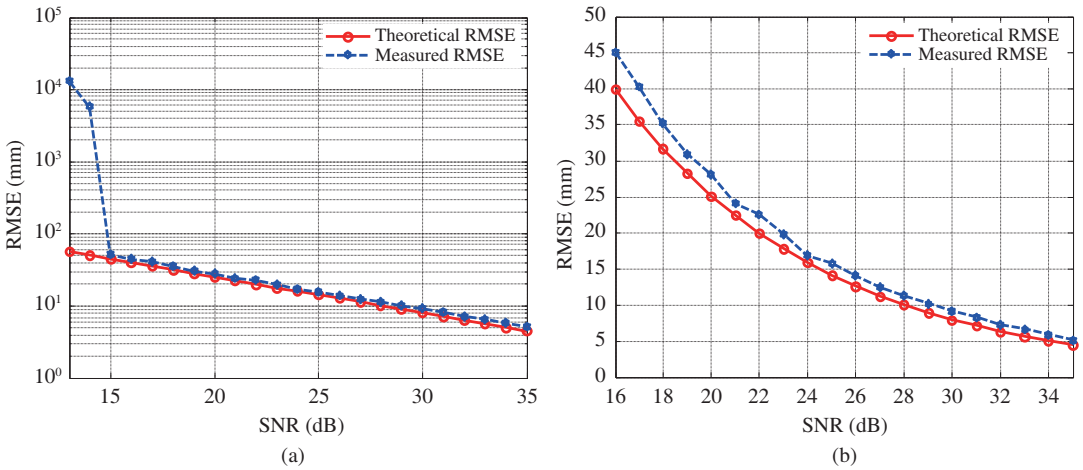

Figure 4 (Color online) Simulated accuracies of EVMs in different SNR environments. (a) SNR range: 13–35 dB; (b) SNR range: 16–35 dB.

error (RMSE) reached the order of centimeters or millimeters in EVM and the order of millimeters or sub-millimeters in PDRM. The detection probability of the target decreased at SNRs below 16 dB. If the detection fails, the EVM and PDRM cannot be analyzed. In practice, when the joint target track information is obtained, PDR can be applied in lower-SNR environments.

Subsequently, the PDVM technique has been applied to ISAR images [59] and micro-motion measurements [35, 60]. We proposed a high-quality method that obtains ISAR images by compensating the target motion using accurate velocity information. The novel ISAR motion compensation approach has been conjugated with the PDVM technique to extract the micro-motion features of the target [35]. The phase error induced by the discrete Fourier transform (DFT) was analyzed in [61], and a novel correction method for the phase unwrapping error under low-SNR conditions was developed in [59].

5 Range-spread target tracking technology

HRR improves the accuracy, amount of target information, and performance of target-tracking in cluttered environments. In addition, tracking with a wideband waveform replaces the narrowband waveform of conventional tracking radars and reduces the waste of radar energy, which is important in radar system design. However, high-range resolution also reduces the SNR and introduces false alarms, placing greater performance demands on the data association module and tracking filtering module during tracking.

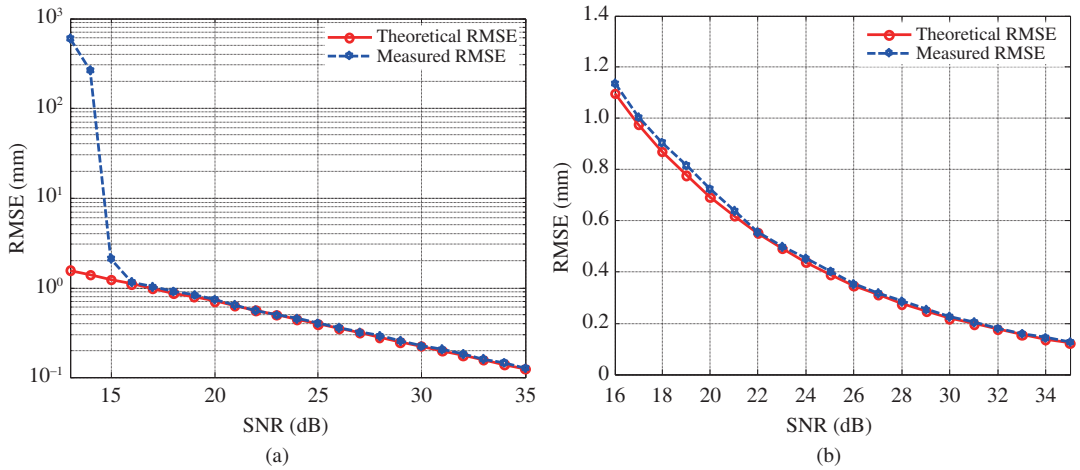

Figure 5 (Color online) Accuracy of PDRMs. (a) SNR range: 13–35 dB; (b) SNR range: 16–35 dB.

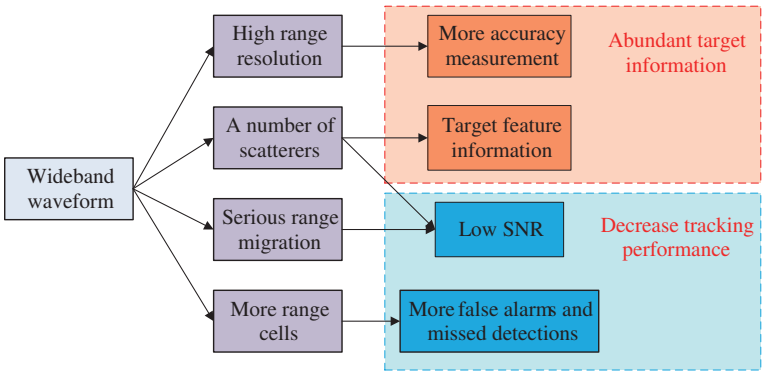

Figure 6 (Color online) Interrelationships among HRR characteristics.

Figure 6 shows the interrelationships among HRR characteristics.

Uncertainties in measurement origins are often reduced by data association algorithms. The typical narrowband tracking theory and its algorithms are based on the point target model. The input observations are used for determining the existing tracks and for initiating a new track [62]. However, HRRs resolve the target into many scattering cells, invalidating the typical narrowband tracking algorithm. The challenge in multiple range-spread target tracking is associating the observations, targets, and tracks. Multiple targets and scattering cells also cause a multiplication of observations, significantly increasing the computation complexity of data association (Figure 7).

5.1 Integrated detection and tracking algorithm

A traditional radar system is split into two independent subsystems-target detection and target tracking [63] – which are implemented in series. In detection, the Neyman-Pearson (NP) criterion is widely used to minimize the false alarm rate and maximize the detection probability. In tracking, the uncertainty in the measurement origin is reduced by data association algorithms such as the probabilistic data association filter (PDAF) [64] and the multiple hypothesis tracker [62]. The traditional detection and tracking algorithm is illustrated in Figure 8.

However, optimizing the subsystems does not necessarily optimize the general system. This topic has attracted the attention of experts globally. To connect the detection and tracking subsystems, some researchers have proposed non-simulation performance prediction (NSPP) methods [65–67]. The performance of the PDAF algorithm has been analyzed by methods based on the modified Riccati equation [65, 66] and the hybrid conditional average (HYCA) [67]. Both methods characterize the impact of false alarms and missed detections during tracking by using the information reduction factor (IRF) [68,69].

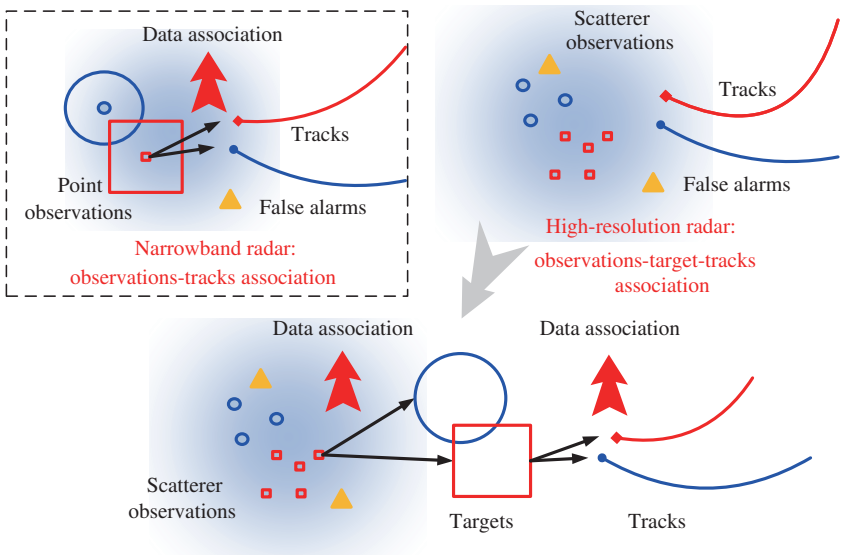

Figure 7 (Color online) Data associations in LRRs and HRRs.

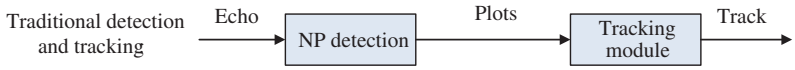

Figure 8 (Color online) Traditional detection and tracking.

In recent efforts, the tracking algorithm based on NP detection has been improved and the joint optimization of detection and tracking has been considered [70]. The optimization parameters in joint optimization are the detection probability and false alarm probability. The filtering performance (filtering covariance) is predicted and the detection parameters are optimized based on the NSPP result.

Besides optimizing the detection threshold, some scholars have also analyzed the influence of radar waveform parameters on the tracking performance, and have proposed several optimization methods for these parameters [71–75]. The authors of [71] proposed a dynamic waveform selection algorithm to strive for tracking error minimisation for manoeuvering target tracking in clutter. The proposed dynamic waveform selection algorithm can improve tracking performance considerably, especially in terms of track loss probability. The authors of [72] combined an autoregressive (AR) model into the Kalman filter for target tracking, and optimized the waveform by minimizing the Cramer–Rao lower bound for estimating the target range. After more in-depth research on this topic, the relevant theoretical results were summarized into a theoretical system of cognitive radar.

Although the above method improves the tracking performance, some major problems must be resolved before the method is feasible in practice. First, IRF cannot be analytically expressed in terms of NP detection. Performance prediction requires a numerical calculation method, which is difficult to adapt to the high requirements of radar data processing in real time. Second, the target-feature information provided by the tracking module is not used in the detection process, meaning that the information flow remains unidirectional.

Quite different to NP detection is Bayesian detection [76–78]. The PDAF algorithm with Bayesian detection (PDAF-BD) [76] feeds back the filtered target-position information to the detection module and introduces a spatial variation threshold, reducing the false alarm rate and improving the detection and tracking performances. The Bayesian detector increases the information interaction between the tracking system modules, which suppresses the number of false alarms and is theoretically suitable for wideband radar. However, the cost of Bayesian detection and the pre-determined threshold of the detector are difficult to estimate. If the detector parameters are not properly selected, the tracking performance will be degraded. This problem largely limits the application of Bayesian detection.

To mitigate these problems, we proposed an HYCA method for the PDAF-BD algorithm [79]. For a

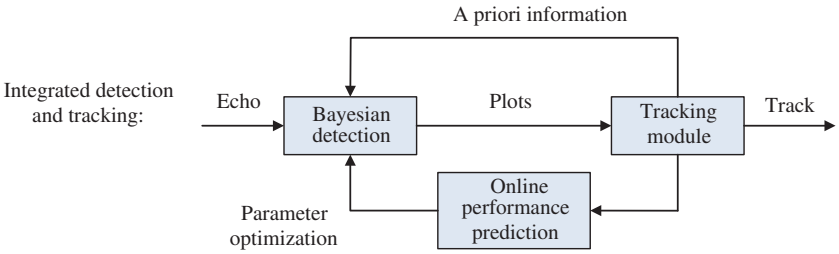

Figure 9 (Color online) Integrated detection and tracking algorithm based on Bayesian detection.

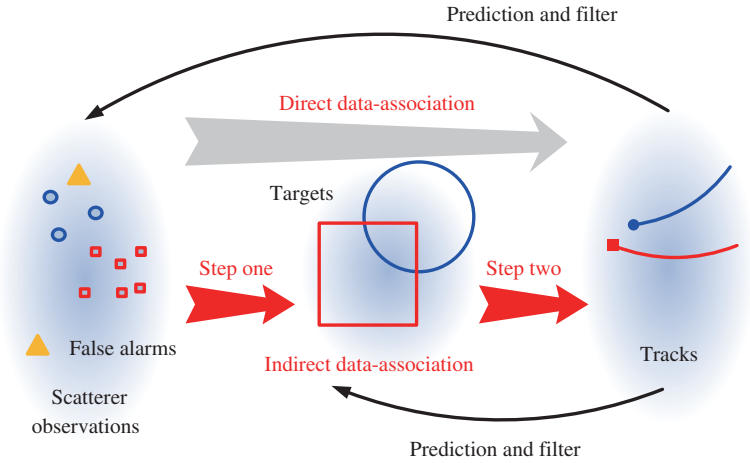

Figure 10 (Color online) Schematic of the range-spread target-data association method.

given scene and algorithm parameters, the HYCA method predicts the track loss probability and errors in the tracking algorithms at different times by observing the number of probability distributions and iterating the computation of the filtering covariance matrix. We also proposed an integrated detection and tracking algorithm based on Bayesian detection, which applies the performance prediction method [80] of the above PDAF-BD algorithm as a sub-module of the tracking algorithm. During the tracking process, the tracking performance under varying detection parameters is predicted from the tracking status of the current frame. The detection parameters are dynamically optimized to maximize the tracking performance. The integrated detection and tracking algorithm based on Bayesian detection is illustrated in Figure 9.

5.2 Multiple target tracking with switching of attribute states

Multi-target tracking (MTT) attempts to relate the tracking to an observation. For this purpose, all possible associated events must be exhaustively considered by a "hard-association" class algorithm. This subsection presents two alternatives to exhaustive searching: indirect data-association and direct data-association. Figure 10 shows the differences between the two methods.

(1) Indirect data-association method. The indirect data-association method reprocesses the range-spread target observations to obtain the center of the multiple scattering cells as the target observation. This method, which constitutes a type of "clustering" processing, is followed by target observation and track association.

Koch [81] proposed a method that associates an observation with a target when the multiple range-spread targets are sparsely distributed. The observation-target association is completed by applying the nearest-neighbor method within an ellipse. Salmond [82] established the object-target affiliation by applying the Bayesian association method on the combined observations.

The range-spread target association method is clear and reduces the computational complexity. Al-

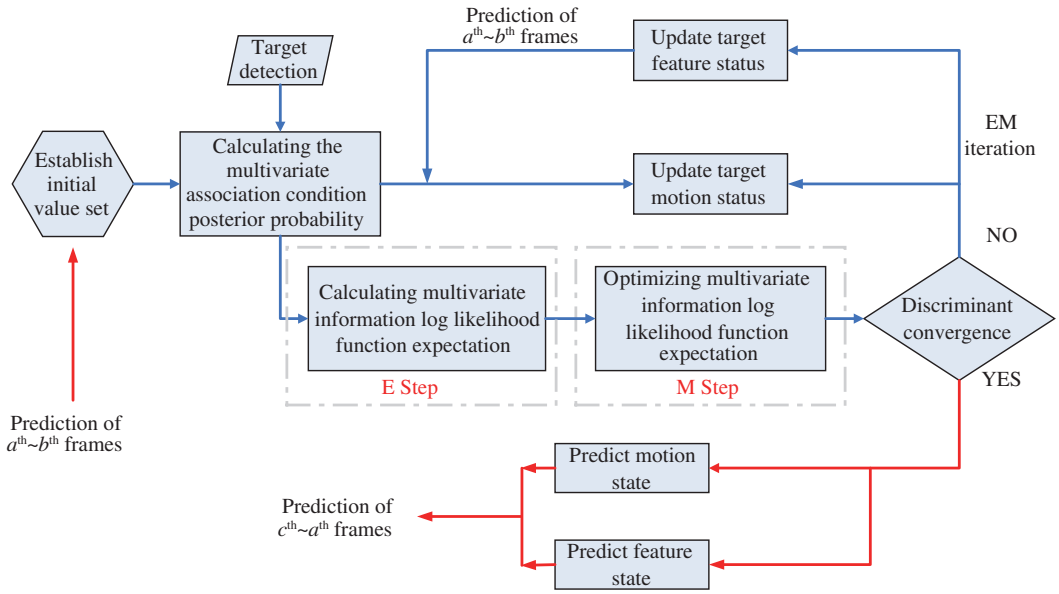

Figure 11 (Color online) Flowchart of the attribute-aided tracking method based on EM.

though the classical multi-target association method directly processes the associated data, it does not form a closed-loop structure; rather, the information flows in the observation-target and target-track associations are unidirectional, meaning that the former cannot obtain the a priori information fed back by the latter. When the numbers of false alarms and missed detections are significant, the observation–target association will largely deviate, decreasing the accuracy of the target-parameter estimation. These errors will accumulate over time and the target-track correlation process will eventually fail. The inability to improve the estimation using the time information, and to ensure the performance of the scattering point–target correlation, are the bottlenecks of the entire association process, restricting the performances of data-association methods to some extent.

(2) Direct data-association method. The direct data-association method assigns multiple observations to a certain track at the same time. The assignment is based on the characteristics of the association between the range-spread target observation and the track [83]. Therefore, such a method is directly extendible to the target- tracking problem of HRRs. The most representative method is the probabilistic multi-hypothesis tracker (PMHT) method based on the expectation maximization (EM) algorithm [84].

Owing to its flexibility and scalability, PMHT has attracted the attention of scholars around the world and PMHT improvements have been actively sought in MTT theory. The accurate measurements and abundant target information of PMHT reduce the number of missed associations and improve the tracking performance. How to assist the association by exploiting the target-feature information is essential for improving the target tracking performance [85, 86]. Previous studies have incorporated the feature information into PMHT [87–97]. In some of these studies [92–94], the target is spatially expanded by the ellipsoid model and the tracking is assisted by the structural information of the target. The PMHT with classification measurements (PMHT-C) method assists the association using the target classification features within the PMHT framework [95, 96]. The attribute measurements and targets are related through a matrix that is independent of time and observations. The method improves the correlation performance when the motion states are blurred.

However, the matrix correlating the measured attributes and target features may change in practice. For example, the observed number of scattering points is not only affected by false alarm detections and fluctuations but also depends on the target attitude. The PMHT-C algorithm cannot cope with switching of the target-feature states, and its performance degrades in this circumstance.

To resolve these problems, an EM-based attribute-aided tracking algorithm has been developed [97]. Figure 11 is a flowchart of this attribute-aided tracking method. The attribute characteristics are de-

scribed by a hidden Markov model and a joint probabilistic model of the kinematic and attribute properties is derived. Based on these derivations, an EM-based iterative algorithm is developed. The kinematic and attribute information in multiple frames is used for association and filtering. The performance of this algorithm improves when the target attributes are available.

6 ISAR imaging technology

The ISAR obtains range-Doppler images of non-cooperative moving targets. For this reason, it has become an attractive option in recent years. Using the relative rotational and translational motions between a target and the radar's line of sight, ISAR reconstructs a two-dimensional high-resolution image of the target. The desired relative motion is uniform rotational motion without translational motion. The undesired translational component causes range migration and phase modulation, both of which degrade the quality of the ISAR image [98,99]. Accordingly, this component is removed by a motion compensation technique.

Complicated movements of a target involve nonuniform rotational motions. Therefore, well-focused ISAR images usually require rotational motion compensation (RMC) [100–108]. Over the past few years, extensive RMC methods have been proposed. ISAR imaging of maneuvering targets is handled by different time-frequency analysis methods [100–103], such as adaptive Doppler spectrum extraction [100], fractional Fourier transform [101], and modified Wigner-Ville transform [102]. In RMC, images can be focused without constructing a parametric rotational motion model and estimating its parameters. Another method is based on the adaptive joint time frequency (AJTF) algorithm [104]. The authors of [104] optimized a cost function using the AJTF algorithm, and then estimated the polynomial phase signal of the dominant scatterer used to remove the target's nonuniform rotational motion. Recently, Kang et al. [106] proposed a new ISAR RMC method that formulates the polynomial phase signal of the dominant scatterer using the polynomial-phase transform. Liu et al. [108] proposed a novel estimation and compensation method that removes the nonuniform rotational motions of maneuvering targets, thereby compensating the nonlinear migration through the range cells and the high-order terms in the range-cell echoes. They constructed a rotational motion model with constant angular acceleration, and analyzed its influence on the image quality. The rotational motion parameters were estimated by particle swarm optimization.

In addition, the unwanted translational motion of the target must be removed by reliable translational motion compensation (TMC) [109–116]. TMC methods, which include Doppler centroid tracking (DCT) [109], phase gradient autofocus (PGA) [110, 111], minimum entropy phase autofocus [112], and maximum contrast phase autofocus [112], estimate and compensate the phase error caused by translational motion. If the target's rotational motion can be ignored and no prominent point exists, the phase error estimation obtained by DCT becomes a maximum likelihood estimation [109]. As the target's rotational motion cannot be ignored and prominent points may exist, the assumptions of DCT may be invalid in real applications. Instead, PGA integrates the information of several prominent scatterers to more precisely estimate the phase error in the translational motion [110]. However, selecting the prominent scatterers is a difficult task. Recently, subspace algorithms based on eigenvalue decomposition (EVD) have been proposed [113–116], which are robust and more effective for ISAR phase autofocus than PGA. More specifically, Cao et al. [113] proposed a minimum-entropy ISAR autofocus algorithm (MESA), which optimizes the weights of the principle eigenvectors by an iterative optimization method, and then estimates the phase error in the translational motion. Suppose that a relatively strong scatterer exists on the target. After constructing the EVD of the covariance matrix from the complex range-aligned echoes, the translational motion phase error can be estimated as the single eigenvector corresponding to the largest eigenvalue. This method is called single eigenvalue autofocus (SEA) [114]. Recently, the efficiency of TMC has been improved by a new concept called eigenimage, which defines the fast Fourier transform output of the principal eigenvectors [115]. However, the methods in [113, 115] require complicated iteration and optimization procedures. In addition, the computational complexity of EVD is of

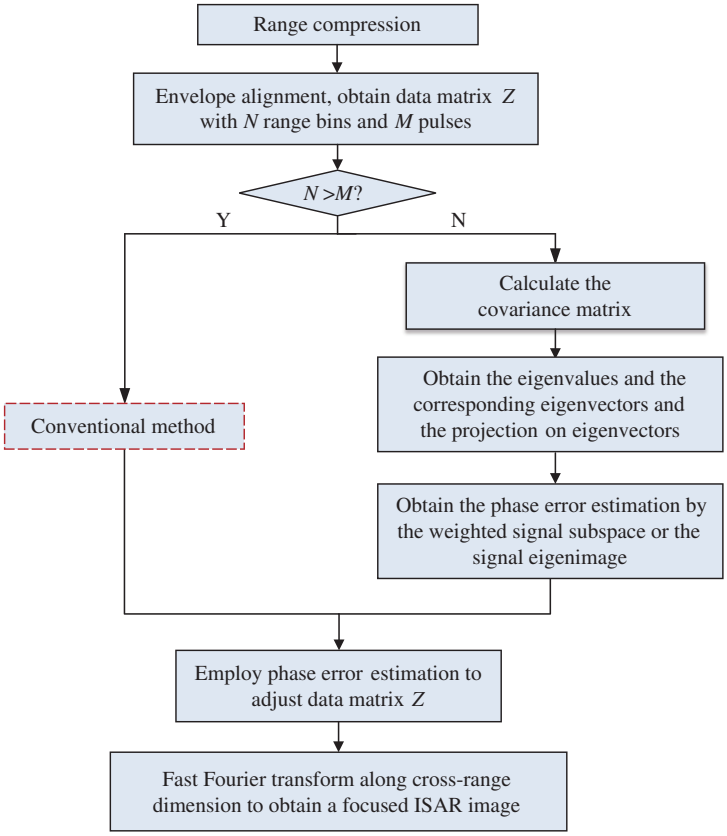

Figure 12 (Color online) Flowchart of the proposed method.

the order of $O(M^3)$, where M is the dimension of the covariance matrix with respect to the number of pulse samples [113–115]. To enhance the cross-range resolution of the given pulse repetition frequency, a larger observation pulse number is usually requested. Consequently, all of the above EVD-based autofocus methods are disadvantaged by the high computational complexity of processing the high-dimensional covariance matrix.

To avoid the high computational complexity of EVD-based autofocus methods, the authors of [116] proposed an alternative approach that generates the covariance matrix more efficiently. First, HRRPs are obtained by compressing the original range. The data are then range-aligned and inserted into a matrix. Subsequently, the numbers of range bins are compared with those of pulse samples. If there are more range bins than pulse samples, the covariance matrix can be constructed by a conventional EVD-based method. Otherwise, the dimension of the covariance matrix can be reduced by transposing the range-aligned data matrix and performing successive phase autofocuses. This approach significantly reduces the computational complexity of EVD. Figure 12 is a flowchart of this alternative method.

Airplane echo data have been recorded by an S-band experimental ISAR system. Using a stepped frequency signal with a synthetic bandwidth of 320 MHz, this experiment collected 256 pulses with an average pulse SNR of 16 dB in the range-aligned data. Figure 13 shows the results of DCT, PGA, and the modified SEA and MESA algorithms (M-SEA and M-MESA, respectively) on these real aircraft data.

The targets in the ISAR images obtained by DCT and PGA (panels (c) and (d) of Figure 13, respectively) are almost merged by noise. The focus qualities of the images obtained by M-MESA and M-SEA (panels (e) and (f) in Figure 13, respectively) are vastly improved. The contrasts of ISAR images obtained by the four methods are compared in Table 2. The higher the contrast, the better is the focus quality. In Table 2, the contrast values of DCT and PGA were lower than those of M-MESA and M-SEA, consistent with the above discussion. Furthermore, M-MESA yielded a better result than M-SEA because M-MESA uses more eigenvectors that contribute to the signal subspace.

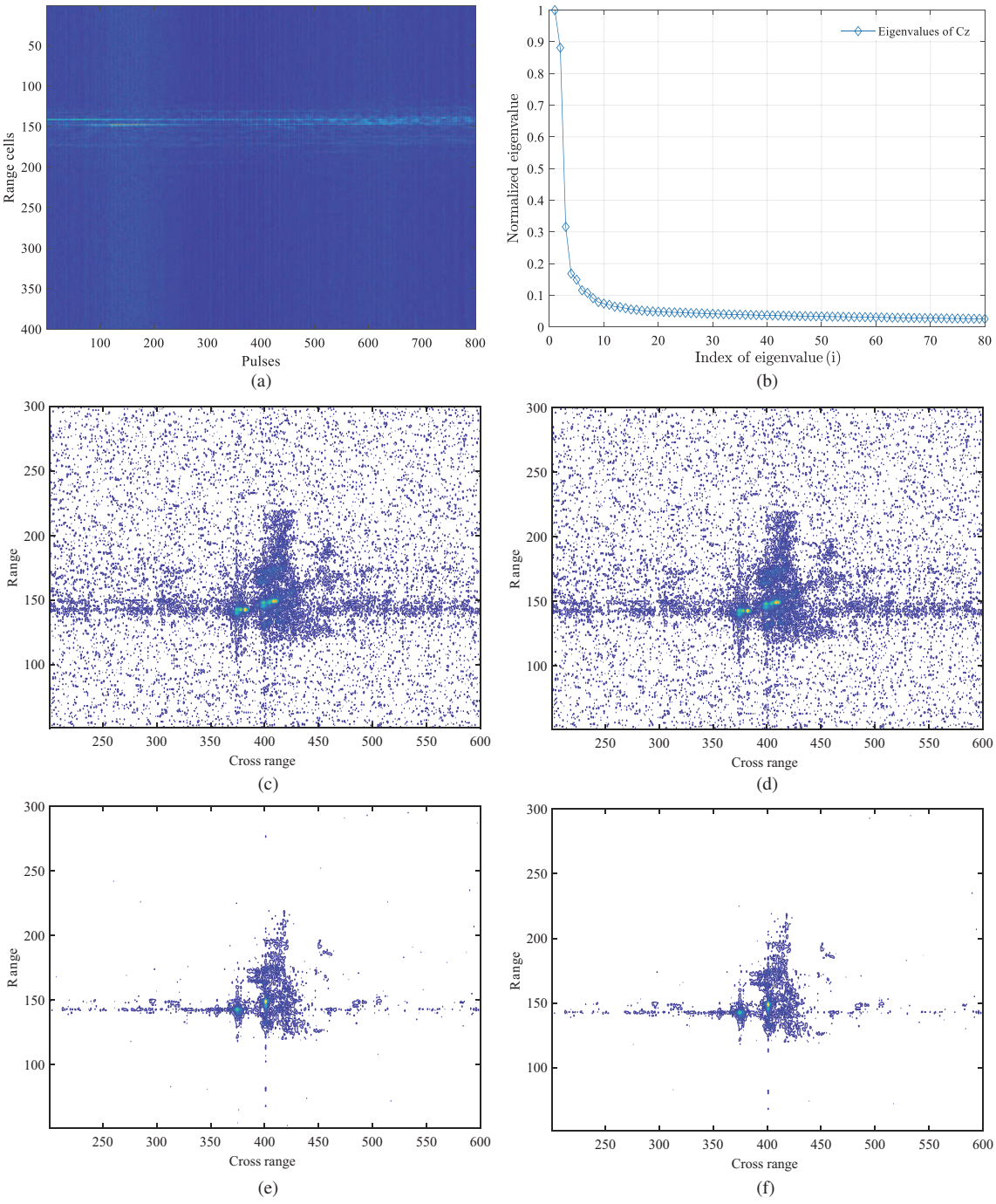

Figure 13 (Color online) Results of measured airplane data. (a) Envelope alignment by ACM; (b) first 80 eigenvalues of the covariance matrix; (c) DCT; (d) PGA; (e) M-SEA; (f) M-MESA.

Table 2 Contrast comparison of different autofocus methods

Method	DCT	PGA	M-SEA	M-MESA
Contrast	10.5218	14.0038	23.9199	24.3422

7 Automatic target recognition technology

Radar automatic target recognition (RATR) is a specific application of the pattern recognition theory in the radar field. RATR extracts the discernible features from the frequency, phase, amplitude, and polarization information of the scattered field echo signals generated by the target in the far field of the

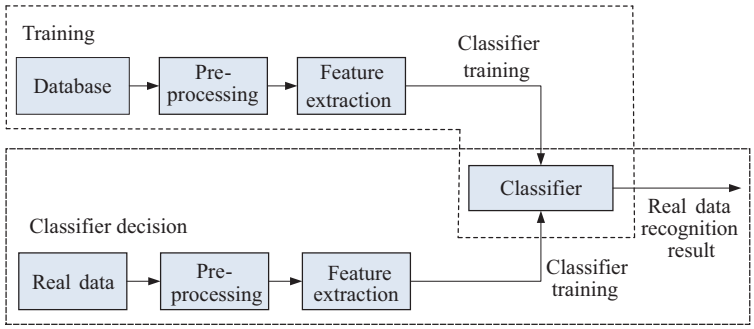

Figure 14 (Color online) Implementation process of radar automatic target recognition.

radar, and identifies the target using the a priori target information [117–121]. A typical RATR system is divided into four modules: data acquisition, preprocessing, feature extraction, and selection (also known as classifier training or decision-making). The data used for identification are divided into training data and real data. The framework of RATR implementation is shown in Figure 14.

The RATR tasks can be classified into the following three levels:

(1) Discrimination of target attributes such as the warheads, number of aircraft in the formation, satellites, and space debris [122].

(2) Determination of the targets, which may be helicopters, propellers, jets, wheeled and tracked vehicles, or other objects.

(3) Determination of the target model, for example, jet aircraft Su-35 and F-22 and ground track vehicles T-90 and M1A2.

RATR is gradually developed from low-level discrimination to high-level classification and identification. In general, the target becomes more difficult to identify as the level increments, requiring more target information and finer images.

7.1 HRRP attitude sensitivity problem

The HRRP of the target is the projection of the target scattering center in the direction of sight. HRRP, which reflects the geometric and structural features of the target, is among the main methods of wideband radar target recognition [117, 123–126]. The echo of each resolution cell of the target's HRRP is formed by superposing the echoes of multiple scattering centers in the resolution cell. When the target position changes relative to the radar's line of sight, the radial range of the scattering center also changes, causing a phase change of the echo. In turn, the phase change alters the vector superposition result and the shape of the HRRP appears to undulate. The sensitivity of HRRP to attitude variations increases with increasing (decreasing) carrying frequency (wavelength) of the wideband radar. When the angle of view varies significantly, the distribution of the scattering center in the sight direction may be significantly changed by the shielding effect, which may distinctly alter the HRRP.

HRRP target recognition must resolve three main problems: orientation sensitivity, translation sensitivity, and amplitude sensitivity. Researchers worldwide have conducted in-depth research on these issues and proposed various solutions.

Orientation sensitivity refers to the notable shape changes in HRRP for small changes in the orientation angle when there is relative rotation between the radar and the target. It is sourced from the relative change in the radial distance of each scattering point on the target, and is the most difficult and critical issue. At present, the main solution is to divide the HRRP sequence into several subsets, each covering a small range of orientation angles. A training template is then constructed for each subset, which can be considered as orientation-insensitive. Orientation sensitivity is usually relaxed by equally spacing the entire azimuthal domain; each angular domain is then analyzed by an analytical mathematical model [127]. The authors of [128] adaptively divided the azimuthal domain using the factor analysis model and the Riemann manifold bending rate model, and calculated the average range profile to achieve target recognition.

Table 3 Typical HRRP features

Feature category		Example
Waveform characteristics	Scale characteristics	Length, number of scattering points
	Fluctuation characteristics	Mean, variance
	Structure characteristics	Symmetry, wave, entropy descaling
Transformation characteristics	Spectral characteristics	Spectrum, bispectrum, high order spectrum
	Multiscale feature	Wavelet transform
	Subspace characteristics	PCA, LLE

The translation sensitivity problem is caused by the relative motion of the target and the radar, meaning that the relative position of the target range migrates within the length of the wave-gate window. Translation sensitivity is usually handled by one of the two methods: (1) alignment method, which mainly involves correlation alignment and absolute alignment, and (2) HRRP translation-invariant features. The commonly used features include the Fourier transform spectrum amplitude, bispectrum features, high-order spectral features [129], and central moment features [130].

The amplitude sensitivity problem refers to the unfairness of the data in the subsequent classification and recognition. This problem is caused by the inconsistency in the magnitude-scale standards of the range image (due to differences between the radar and the target range, transmission power, antenna gain, and other uncontrollable phenomena). It is commonly solved by normalizing the amplitude based on measured criteria or by searching for the optimal amplitude-matching factor.

7.2 Hierarchical target recognition algorithm

In general, radar target recognition consists of two steps: feature extraction and classification. Feature extraction isolates a set of features representing the essential attributes of the target from HRRP. Feature classification maps the feature set to the corresponding class of the target by machine learning [117–130].

Feature extraction must identify the information reflecting the essential attributes of the target, which form the basis of the classification. Table 3 shows the commonly employed features in HRRP recognition. The waveform features directly reflect the shape of HRRP. Typical waveform features include the scale, statistical, and structural features. The scale features reflect the radial length, number of scattering centers, and other scale properties of the target. The statistical features reflect the amplitude change information, and the structural features reflect the spatial distribution information of the scattering center. The transformation features are extracted by a specific transform of HRRP. The spectral and multi-scale features are obtained by a transform function (such as a Fourier or bispectrum transform) and a wavelet transform, respectively, and the subspace characteristics are formed by dimensionality reduction methods such as principal component analysis (PCA) and local linear embedding.

However, the traditional HRRP feature-extraction method requires advanced human experience, and a universal set of features is difficult to form. In specific applications, feature extraction and selection often consume much manpower and time, largely restricting the application of HRRP recognition.

In multi-feature recognition, we need to select the appropriate feature subset and construct the corresponding classifier that recognizes different targets in different environments. If all features are fused blindly, the dimension of the feature vector will be greatly increased, which not only increases the computation effort and storage but may also reduce the recognition performance. Moreover, features differ in their physical meanings and usages.

A hierarchical recognition method handles different features by different classifiers. When designing classifiers at different levels, the classifier must be optimized by considering the physical meanings and statistical distributions of the features. For example, features such as target size and scattering center can be classified by a simple threshold discriminant classifier or a decision tree classifier, whereas the structural and statistical features of the scattering centers can be discriminated by a support vector machine classifier. Before making the final decision, the results of different classifiers can be combined by an ensemble classification method.

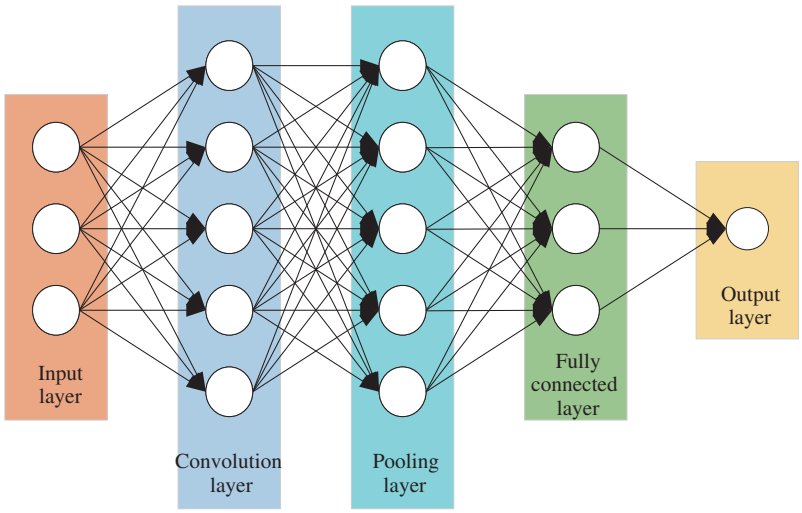

Figure 15 (Color online) HRRP recognition using a convolution neural network.

Table 4 Parameters of the X-band high-resolution monopulse precision-tracking test radar

Parameter	Value
Frequency band	X
Signal bandwidth	1 GHz
Peak power	4 kW
Antenna aperture	2.5 m
Azimuth	0°–360°
Elevation	−3°–180°

For adaptive feature extraction, we can exploit the end-to-end capability of deep neural networks. Deep learning avoids the high dependence of the traditional machine learning algorithm on human experience [118–121]. Deep neural networks include deep autoencoders, deep convolution neural networks, and deep recurrent neural networks. Among these, the deep convolution neural network is most commonly used. Figure 15 is a block diagram of HRRP recognition using a deep convolution neural network. The network includes a convolution layer, a pooling layer, and a fully connected layer. The stacked convolution layer and pooling layer map the original data directly to the high-level abstract features, which are then mapped to the target through the fully connected layer. The entire process requires no human intervention.

8 Applications of HRR

8.1 High-resolution monopulse precision-tracking test radar

Based on theoretical research of HRR algorithms, the Beijing Institute of Technology has developed an X-band high-resolution monopulse precision-tracking test radar. The main parameters of the system are shown in Table 4. In January 2016, the wideband test radar successfully realized full-bandwidth closed-loop tracking of civil aircraft in real time, and verified the key technologies of signal processing and data processing in wideband detection, tracking, high-precision measurement, imaging, and other procedures. As an important test platform, the wideband radar provides continuously measured data support for subsequent wideband detection and tracking research. Figure 16 is a photograph of the X-band wideband test radar.

The X-band wideband radar records the echo data of an Airbus A320 airplane. The bandwidth of the wideband signal is 500 MHz. Initially, the radar system is led to the target by optical or ADS-B guidance. Once the radar system has captured the target, it switches to monopulse automatic tracking.

Figure 16 (Color online) Photograph of the X-band high-resolution monopulse precision-tracking test radar.

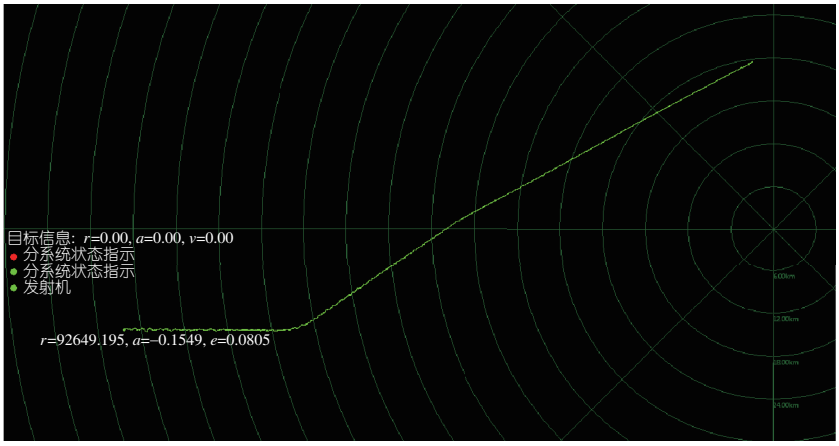

Figure 17 (Color online) Real-time closed-loop tracking of a civil aircraft.

Figure 17 demonstrates the real-time closed-loop tracking of the civil aircraft. The maximum detection range of the target exceeded 90 km, implying that the aircraft was successfully tracked. This result justifies the use of signal-processing technology in wideband detection and tracking.

The envelope velocities and phase-derived velocities measured over 12 s, obtained from 2048 frames of airplane echo data, are plotted in panel (a) of Figures 18 and 19, respectively. Panel (b) of each figure plots the velocity fluctuation error, defined as the difference between the measured data (blue plot) and the least-squares fitting result (red line). The RMSEs of the EVM and PDVM are 2.3 and 0.055 m/s, respectively.

The adjustment amount required for envelope alignment was computed from the PDVM results of frames 513–768 in the ISAR echo data. The ISAR imaging results of the civil aircraft were obtained after TMC and are plotted in Figure 20.

8.2 Foreign object debris high-resolution radar

Wideband radar target-recognition technology can detect foreign object debris (FOD) on airport runways. FOD defines any foreign material, debris, or object that may damage the aircraft in the operational airport area. If not removed, FOD can damage the aircraft at the most critical stage of the flight (taxiing and takeoff), resulting in catastrophic losses.

Traditional FOD detection relies on human vision, which is poor-quality and inefficient. The flight capacity can be improved by installing photoelectric equipment, but such automated photo-detection is degraded by bad weather conditions (such as rain, fog, and haze). In recent years, the millimeter wave (MMW) radar has shown promising performance in FOD detection. MMW radar operates under both daytime and nighttime conditions, is highly sensitive to small foreign objects, has high positioning

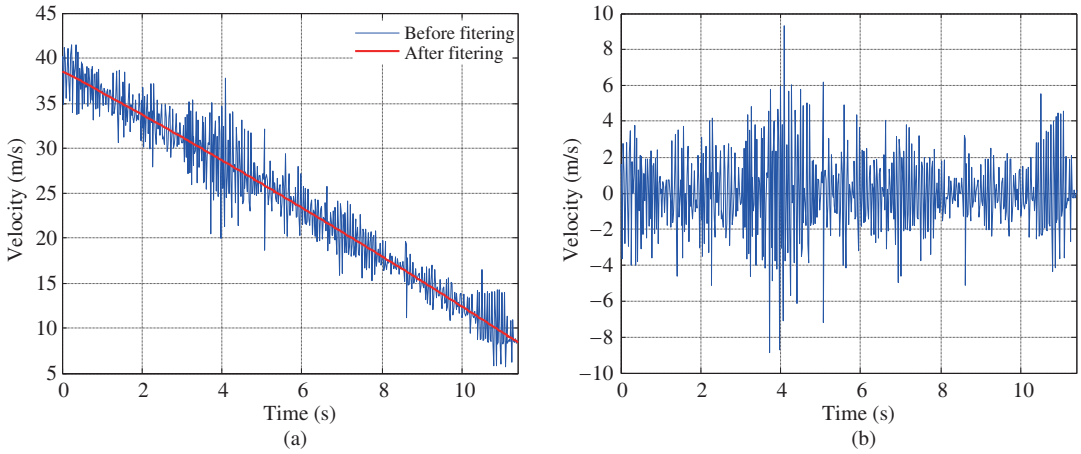

Figure 18 (Color online) Analysis of the measured civil aircraft envelope velocities. (a) Velocity measurements; (b) velocity fluctuation errors.

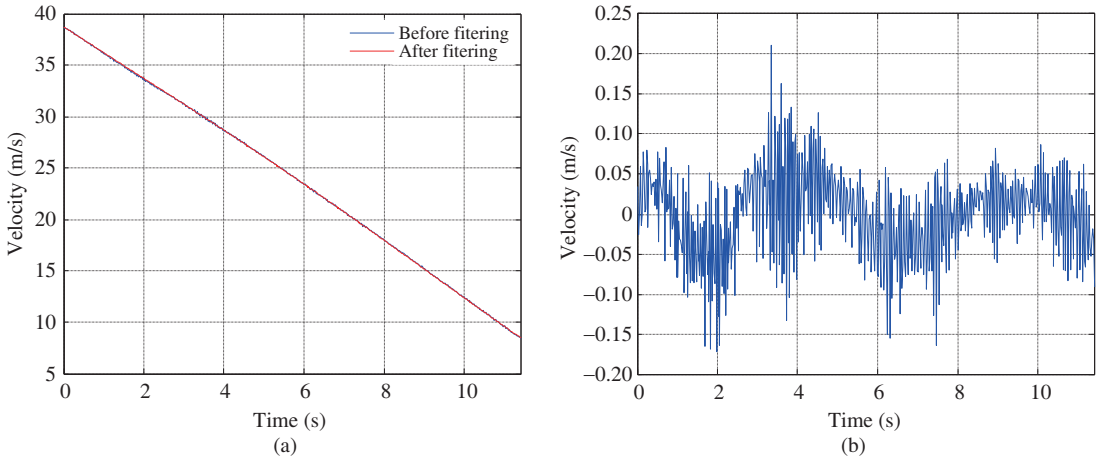

Figure 19 (Color online) Analysis of the phase-derived velocity measurements of the civil aircraft. (a) Velocity measurements; (b) velocity fluctuation errors.

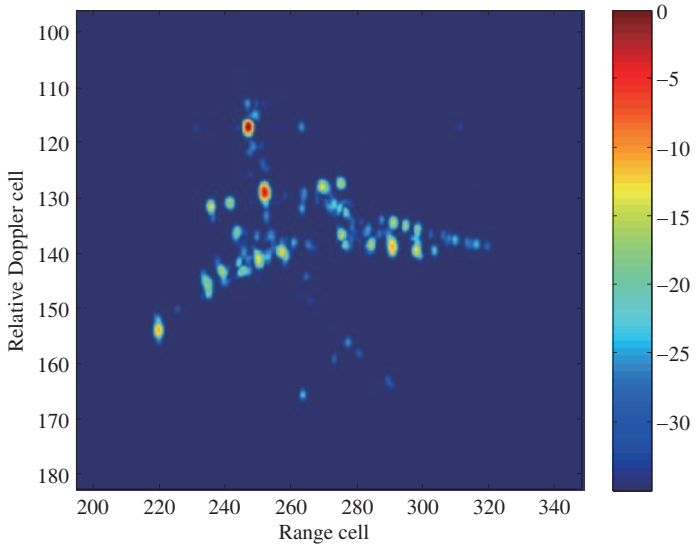

Figure 20 (Color online) ISAR imaging results of the civil aircraft.

Figure 21 (Color online) FOD radar.

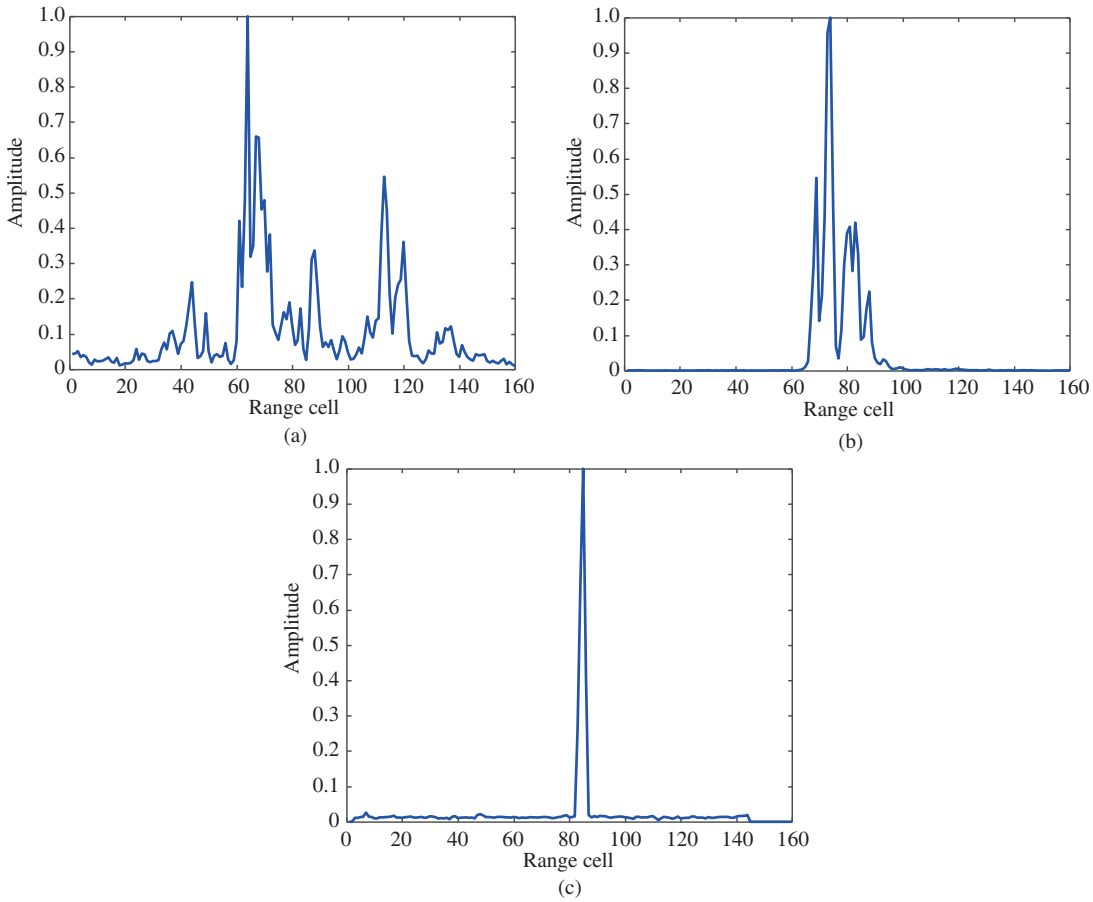

Figure 22 (Color online) One-dimensional images captured by FOD radar on an airfield. (a) Aircraft; (b) vehicles; (c) foreign objects.

accuracy for both distance and angle, and is strongly adaptable to bad-weather conditions. Moreover, when combined with photoelectric equipment and Beidou positioning equipment, the MMW radar can position and report FOD with high accuracy and high speed, greatly improving the quality and efficiency of detection, and hence, the safety and navigation ability of the airport operation.

The FOD detection radar developed by the Beijing Institute of Technology is a high-resolution W-band radar using a linear frequency-modulated continuous wave, as shown in Figure 21.

Panels (a), (b), and (c) of Figure 22 show the measured HRRPs of the aircraft, ground vehicles, and foreign objects, respectively. These objects can be distinguished by their scale-structure characteristics,

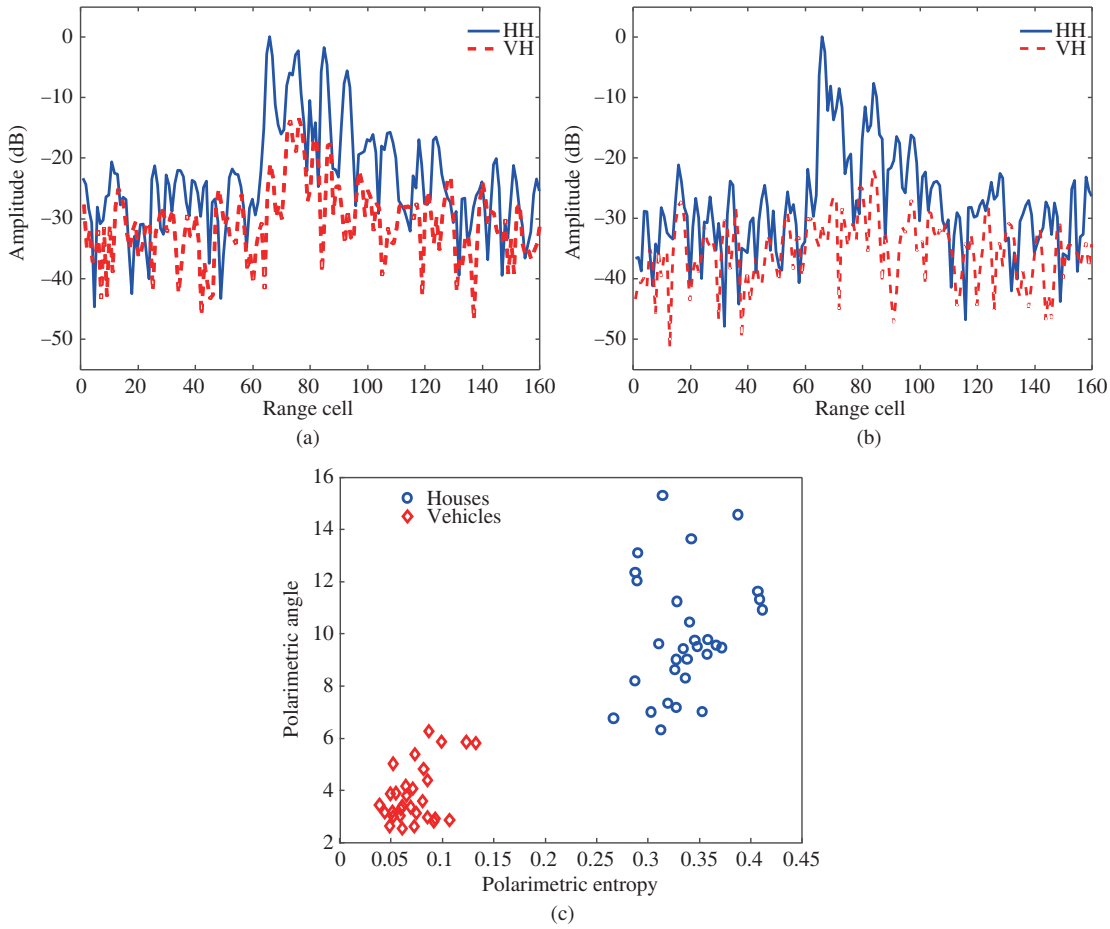

Figure 23 (Color online) Measured dual-polarized one-dimensional images of houses (a) and vehicles (b), and their polarization features (c).

realizing automatic target recognition.

8.3 Dual polarization high-resolution radar

Combined with polarization measurements, high-resolution imaging technology can capture the distribution of the "spatial-polarimetric" scattering characteristics of a target. From this information, one can extract the spatial structure of the target and the characteristics of polarization scattering, and form the shape features of the target structure. This dual technology holds great potential in radar target recognition [131–133].

Polarization measurement methods are divided into full polarization and dual polarization modes. Full polarization obtains the whole polarimetric scattering matrix, but requires complex hardware, waveform design, and signal processing. At present, full polarization has been applied in spaceborne SAR, shipborne radars, and GBRs.

The dual polarization mode measures a single column of the target polarization scattering matrix. Although dual polarization provides less information than the full polarization radar, it provides more target information than traditional single-polarization radar while reducing the hardware complexity of the system. The dual polarized high-resolution radar developed by the Beijing Institute of Technology uses a stepped frequency chirp signal in the W-band [134]. The maximum synthetic bandwidth is 1.2 GHz. Figure 23 shows the dual polarized HRRPs and polarization characteristics of houses and vehicles collected by this radar. The HRRPs of both targets have certain similarities and are difficult to distinguish with reliability. However, their extracted polarization features are well separated, meaning that both targets are reliably identified in the dual polarization mode.

9 Summary and prospects

HRRs can potentially improve the detection ability of space targets in complicated environments. They improve the accuracy of target detection, obtain more feature information of the target, and are more aware of the environment than traditional radars, highlighting the feasibility of diverse and intelligent signal processing algorithms in radar applications. However, to satisfy diverse military and civilian needs, HRR performance must be further improved.

This paper reviewed the latest research on HRRs, including target detection, tracking, imaging, and recognition by HRRs. It also discussed the relevant issues and solutions and analyzed the representative HRR systems, exemplifying them by experimental results. An HRR efficiently suppresses the target RCS fluctuations, angular glint, clutter, and other interferences, and is regarded as the direction of radar research and development. However, its resolution remains insufficient for general applications and the bandwidth should suit the scattering characteristics of the specific target. Resolving these problems will be the focus of future research.

Judging from the existing methods of high-resolution signal processing, we anticipate that more attractive and effective methods will be proposed in the future, enabling the HRR tracking of complex targets in complex environments. Innovations in this field will boost the development and applicability of HRRs.

Acknowledgements This work was supported by National Natural Science Foundation of China (Grant No. 61771050) and 111 Project of the China Ministry of Education (MOE) (Grant No. B14010).

References

1 Fabrizio G A. High Frequency Over-the-Horizon Radar: Fundamental Principles, Signal Processing, and Practical Applications. New York: McGraw-Hill, 2013
2 van Trees H L. Detection, Estimation, and Modulation Theory, Part IV: Optimum Array Processing. Hoboken: Wiley & Sons, 2002
3 Farina A. Antenna-Based Signal Processing Techniques for Radar Systems. Norwood: Artech House, 1992
4 Fenn A J, Temme D H, Delaney W P, et al. The development of phased-array radar technology. Lincoln Lab J, 2000, 12: 321–340
5 Brookner E. Phased arrays around the world-progress and future trends. In: Proceedings of IEEE International Symposium on Phased Array Systems and Technology, 2003
6 Wang D C. Discussion on the theoretical foundation of development and innovation for radar technical system. Modern Radar, 2014, 26: 142–148
7 North D O. An analysis of the factors which determine signal/noise discrimination in pulsed-carrier systems. Proc IEEE, 1963, 51: 1016–1027
8 Woodward P M. Probability and Information Theory with Application to Radar. London: Pergamon Press, 1953
9 Dicke R H. Object detection system. US Patent, 2624876, 1953
10 Shirman Y D, Leshchenko S P, Orlenko V M. Advantages and problems of wideband radar. In: Proceedings of IEEE International Radar Conference, Portland, 2003. 15–21
11 Wehner D R. High Resolution Radar. Norwood: Artech House, 1995
12 Eaves J L, Reedy E K. Principles of Modern Radar. New York: Van Nostrand Reinhold, 2010
13 Le Chevalier F. Principles of Radar and Sonar Signal Processing. Norwood: Artech House, 2002
14 Long T, Liu Q H, Chen X L. Wideband Radar. Beijing: National Defense Industry Press, 2017
15 Lindsay J E. Angular glint and the moving, rotating, complex radar target. IEEE Trans Aerosp Electron Syst, 1968, 4: 164–173
16 Barton D K. Radar system analysis and modeling. IEEE Aerosp Electron Syst Mag, 2005, 20: 23–25
17 Skolnik M I. Radar Handbook. 3rd ed. New York: McGraw-Hill, 2008
18 Brookner E. Aspects of Modern Radar. Norwood: Artech House, 1988
19 Li N J, Zhang Y T. A survey of radar ECM and ECCM. IEEE Trans Aerosp Electron Syst, 1995, 31: 1110–1120
20 Greco M, Gini F, Farina A. Radar detection and classification of jamming signals belonging to a cone class. IEEE Trans Signal Process, 2008, 56: 1984–1993
21 Howard D. High range-resolution monopulse tracking radar. IEEE Trans Aerosp Electron Syst, 1975, 11: 749–755
22 Rycroft M J. Book review: understanding synthetic aperture radar images. J Atmos Sol-Terr Phys, 1999, 61: 424
23 Zeng T, Liu T D, Ding Z G, et al. A novel DEM reconstruction strategy based on multi-frequency InSAR in highly sloped terrain. Sci China Inf Sci, 2017, 60: 088301
24 Li Y C, Jin Y Q. Target decomposition and recognition from wide-angle SAR imaging based on a Gaussian amplitude-phase model. Sci China Inf Sci, 2017, 60: 062305
25 Hu C, Li Y H, Dong X C, et al. Optimal 3D deformation measuring in inclined geosynchronous orbit SAR differential interferometry. Sci China Inf Sci, 2017, 60: 060303

26 Fuster R M, Usón M F, Ibars A B. Interferometric orbit determination for geostationary satellites. Sci China Inf Sci, 2017, 60: 060302
27 Zheng W J, Hu J, Zhang W, et al. Potential of geosynchronous SAR interferometric measurements in estimating three-dimensional surface displacements. Sci China Inf Sci, 2017, 60: 060304
28 Yin W, Ding Z G, Lu X J, et al. Beam scan mode analysis and design for geosynchronous SAR. Sci China Inf Sci, 2017, 60: 060306
29 Ding Z G, Xiao F, Xie Y Z, et al. A modified fixed-point chirp scaling algorithm based on updating phase factors regionally for spaceborne SAR real-time imaging. IEEE Trans Geosci Remote Sens, 2018, 56: 7436–7451
30 Steudel F. An improved process for phase-derived-range measurements. World Intellectual Property Organization, WO 2005/017553 A1, 2005
31 Steudel F. Process for phase-derived range measurements. US Patent, WO 2005/030222 A1, 2005
32 Song C, Wu Y R, Zhou L J, et al. A multicomponent micro-Doppler signal decomposition and parameter estimation method for target recognition. Sci China Inf Sci, 2019, 62: 029304
33 Li K, Liang X J, Zhang Q, et al. Micro-Doppler signature extraction and ISAR imaging for target with micromotion dynamics. IEEE Geosci Remote Sens Lett, 2011, 8: 411–415
34 Liu Y X, Zhu D K, Li X, et al. Micromotion characteristic acquisition based on wideband radar phase. IEEE Trans Geosci Remote Sens, 2014, 52: 3650–3657
35 Guo L Y, Fan H Y, Liu Q H, et al. Analysis of micro-motion feature in ISAR imaging via phase-derived velocity measurement technique. In: Proceedings of IEEE Radar Conference, Seattle, 2017. 0783–0787
36 Roth K R, Austin M E, Frediani D J, et al. The Kiernan reentry measurements system on Kwajalein Atoll. Lincoln Lab J, 1989, 2: 247–276
37 Xia X W, Jing W X, Li C Y. Assessment on GMD's deployment status and operational capability. Mod Defence Technol, 2008, 36: 11–18
38 Zhou W X. Development and prospect of ISAR imaging system and imaging technique. Mod Radar, 2012, 34: 1–7
39 Gerlach K. Spatially distributed target detection in non-Gaussian clutter. IEEE Trans Aerosp Electron Syst, 1999, 35: 926–934
40 He Y, Gu X F, Jian T, et al. A M out of N detector based on scattering density. In: Proceedings of IET International Radar Conference, Guilin, 2009
41 Chen X L, Wang L, Liu S L. Research on extended target detection for high resolution radar (in Chinese). Sci Sin Inform, 2012, 42: 1007–1018
42 Conte E, de Maio A, Ricci G. GLRT-based adaptive detection algorithms for range-spread targets. IEEE Trans Signal Process, 2001, 49: 1336–1348
43 Conte E, de Maio A. Distributed target detection in compound-Gaussian noise with Rao and Wald tests. IEEE Trans Aerosp Electron Syst, 2003, 39: 568–582
44 Bandiera F, de Maio A, Greco A S, et al. Adaptive radar detection of distributed targets in homogeneous and partially homogeneous noise plus subspace interference. IEEE Trans Signal Process, 2007, 55: 1223–1237
45 He Y, Jian T, Su F G, et al. Novel range-spread target detectors in non-Gaussian clutter. IEEE Trans Aerosp Electron Syst, 2010, 46: 1312–1328
46 Dai F Z, Liu H W, Shui P L, et al. Adaptive detection of wideband radar range spread targets with range walking in clutter. IEEE Trans Aerosp Electron Syst, 2012, 48: 2052–2064
47 Jian T, He Y, Su F, et al. Cascaded detector for range-spread target in non-Gaussian clutter. IEEE Trans Aerosp Electron Syst, 2012, 48: 1713–1725
48 Aubry A, de Maio A, Pallotta L, et al. Radar detection of distributed targets in homogeneous interference whose inverse covariance structure is defined via unitary invariant functions. IEEE Trans Signal Process, 2013, 61: 4949–4961
49 Ciuonzo D, de Maio A, Orlando D. A unifying framework for adaptive radar detection in homogeneous plus structured interference – part II: detectors design. IEEE Trans Signal Process, 2016, 64: 2907–2919
50 Shui P L, Liu H W, Bao Z. Range-spread target detection based on cross time-frequency distribution features of two adjacent received signals. IEEE Trans Signal Process, 2009, 57: 3733–3745
51 Xu S W, Shui P L, Yan X Y. CFAR detection of range-spread target in white Gaussian noise using waveform entropy. Electron Lett, 2010, 46: 647–649
52 Xu S W, Shui P L. Range-spread target detection in white Gaussian noise via two-dimensional non-linear shrinkage map and geometric average integration. IET Radar Sonar Navig, 2012, 6: 90–98
53 Shui P L, Xu S W, Liu H W. Range-spread target detection using consecutive HRRPs. IEEE Trans Aerosp Electron Syst, 2011, 47: 647–665
54 Zuo L, Li M, Zhang X W, et al. CFAR detection of range-spread targets based on the time-frequency decomposition feature of two adjacent returned signals. IEEE Trans Signal Process, 2013, 61: 6307–6319
55 Long T, Zheng L, Li Y, et al. Improved double threshold detector for spatially distributed target. IEICE Trans Commun, 2012, 95: 1475–1478
56 Luo Y, Zhang Q, Qiu C W, et al. Micro-Doppler effect analysis and feature extraction in ISAR imaging with stepped-frequency chirp signals. IEEE Trans Geosci Remote Sens, 2010, 48: 2087–2098
57 Zhu D K, Liu Y X, Huo K, et al. A novel high-precision phase-derived-range method for direct sampling LFM radar. IEEE Trans Geosci Remote Sens, 2016, 54: 1131–1141
58 Fan H Y, Ren L X, Long T, et al. A high-precision phase-derived range and velocity measurement method based on

synthetic wideband pulse Doppler radar. Sci China Inf Sci, 2017, 60: 082301
59 Fan H Y, Ren L X, Mao E K, et al. A high-precision method of phase-derived velocity measurement and its application in motion compensation of ISAR imaging. IEEE Trans Geosci Remote Sens, 2018, 56: 60–77
60 Fan H Y, Ren L X, Mao E K. A micro-motion measurement method based on wideband radar phase derived ranging. In: Proceedings of IET International Radar Conference, Xi'an, 2013
61 Guo L Y, Fan H Y, Liu Q H, et al. A novel high-accuracy phase-derived velocity measurement method for wideband LFM radar. IEEE Geosci Remote Sens Lett, 2018. doi: 10.1109/LGRS.2018.2879491
62 Blackman S S. Multiple hypothesis tracking for multiple target tracking. IEEE Aerosp Electron Syst Mag, 2004, 19: 5–18
63 Aslan M S, Saranlı A. A tracker-aware detector threshold optimization formulation for tracking maneuvering targets in clutter. Signal Process, 2011, 91: 2213–2221
64 Barshalom Y, Daum F, Huang J. The probabilistic data association filter. IEEE Control Syst, 2009, 29: 82–100
65 Boers Y, Driessen H. Results on the modified Riccati equation: target tracking applications. IEEE Trans Aerosp Electron Syst, 2006, 42: 379–384
66 Brekke E F, Hallingstad O, Glattetre J. The modified Riccati equation for amplitude-aided target tracking in heavy-tailed clutter. IEEE Trans Aerosp Electron Syst, 2011, 47: 2874–2886
67 Li X R, Bar-Shalom Y. Stability evaluation and track life of the PDAF for tracking in clutter. IEEE Trans Autom Control, 1991, 36: 588–602
68 Zhang X, Willett P, Bar-Shalom Y. Dynamic cramer-rao bound for target tracking in clutter. IEEE Trans Aerosp Electron Syst, 2005, 41: 1154–1167
69 Bar-Shalom Y, Zhang X, Willett P. Simplification of the dynamic Cramér-Rao bound for target tracking in clutter. IEEE Trans Aerosp Electron Syst, 2011, 47: 1481–1482
70 Aslan M S, Saranlı A, Baykal B. Tracker-aware adaptive detection: an efficient closed-form solution for the Neyman-Pearson case. Digit Signal Process, 2010, 20: 1468–1481
71 Qin Y L, Wang H Q, Wang J T, et al. Dynamic waveform selection for manoeuvering target tracking in clutter. IET Radar Sonar Nav, 2013, 7: 815–825
72 Jin B, Su T, Zhang W, et al. Joint optimization of predictive model and transmitted waveform for extended target tracking. In: Proceedings of International Conference on Signal Processing, Hangzhou, 2014. 1914–1918
73 Cabrera J B. Tracker-based adaptive schemes for optimal waveform selection. In: Proceedings of IEEE Radar Conference, Cincinnati, 2014. 0298–0302
74 Kyriakides I, Morrell D, Papandreou-Suppappola A. Adaptive highly localized waveform design for multiple target tracking. EURASIP J Adv Signal Process, 2012, 2012: 180
75 Nguyen N H, Dogancay K, Davis L M, et al. Joint transmitter waveform and receiver path optimization for target tracking by multistatic radar system. In: Proceedings of IEEE Signal Processing Workshop on Statistical Signal Processing, Gold Coast, 2014. 444–447
76 Willett P, Niu R X, Barshalom Y. A modified PDAF based on a Bayesian detector. In: Proceedings of American Control Conference, Chicago, 2000. 2230–2234
77 Willett P, Niu R, Bar-Shalom Y. Integration of Bayes detection with target tracking. IEEE Trans Signal Process, 2001, 49: 17–29
78 Aslan M S, Saranli A. Threshold optimization for tracking a nonmaneuvering target. IEEE Trans Aerosp Electron Syst, 2011, 47: 2844–2859
79 Zeng T, Zheng L, Li Y, et al. Offline performance prediction of PDAF with Bayesian detection for tracking in clutter. IEEE Trans Signal Process, 2013, 61: 770–781
80 Zheng L, Zeng T, Liu Q H, et al. Optimization and analysis of PDAF with Bayesian detection. IEEE Trans Aerosp Electron Syst, 2016, 52: 1986–1995
81 Koch J W. Bayesian approach to extended object and cluster tracking using random matrices. IEEE Trans Aerosp Electron Syst, 2008, 44: 1042–1059
82 Salmond D J. Mixture reduction algorithms for point and extended object tracking in clutter. IEEE Trans Aerosp Electron Syst, 2009, 45: 667–686
83 Ceylan S, Efe M. Performance of PMHT based algorithms for underwater target tracking. In: Proceedings of Signal Processing and Communications Applications Conference, Antalya, 2009. 89–92
84 Streit R L, Luginbuhl T E. A probabilistic multi-hypothesis tracking algorithm without enumeration and pruning. In: Proceedings of the 6th Joint Service Data Fusion Symposium, 1993. 1015–1024
85 Drummond O E. Integration of features and attributes into target tracking. In: Proceedings of International Society for Optical Engineering, 2000. 610–622
86 Drummond O E. On categorical feature-aided target tracking. In: Proceedings of International Society for Optical Engineering, 2004. 544–558
87 Wieneke M, Koch W. Probabilistic tracking of multiple extended targets using random matrices. In: Proceedings of International Society for Optical Engineering, 2010
88 Willett P, Coraluppi S. MLPDA and MLPMHT applied to some MSTWG data. In: Proceedings of International Conference on Information Fusion, 2006
89 Georgescu R, Willett P. Predetection fusion with Doppler measurements and amplitude information. IEEE J Ocean Eng, 2012, 37: 56–65
90 Challa S, Pulford G W. Joint target tracking and classification using radar and ESM sensors. IEEE Trans Aerosp

Electron Syst, 2001, 37: 1039–1055
91 Lu Q, Domrese K, Willett P, et al. A bootstrapped PMHT with feature measurements. IEEE Trans Aerosp Electron Syst, 2017, 53: 2559–2571
92 Feldmann M, Franken D. Tracking of extended objects and group targets using random matrices: a new approach. In: Proceedings of International Conference on Information Fusion, 2008
93 Feldmann M, Franken D, Koch W. Tracking of extended objects and group targets using random matrices. IEEE Trans Signal Process, 2011, 59: 1409–1420
94 Lan J, Li X R. Tracking of extended object or target group using random matrix – part II: irregular object. In: Proceedings of International Conference on Information Fusion, 2012. 2185–2192
95 Davey S, Gray D, Streit R. Tracking, association, and classification: a combined PMHT approach. Digit Signal Process, 2002, 12: 372–382
96 Davey S, Gray D. Integrated track maintenance for the PMHT via the hysteresis model. IEEE Trans Aerosp Electron Syst, 2007, 43: 93–111
97 Long T, Zheng L, Chen X L, et al. Improved probabilistic multi-hypothesis tracker for multiple target tracking with switching attribute states. IEEE Trans Signal Process, 2011, 59: 5721–5733
98 Lu G Y, Bao Z. Compensation of scatterer migration through resolution cell in inverse synthetic aperture radar imaging. IEE Proc Radar Sonar Navig, 2000, 147: 80–85
99 Chen V C, Martorella M. Inverse Synthetic Aperture Radar Imaging: Principles, Algorithms and Applications. Edison: SciTech Publishing, 2014
100 Fan L, Shi S, Liu Y, et al. A novel range-instantaneous-Doppler isar imaging algorithm for maneuvering targets via adaptive Doppler spectrum extraction. Prog Electrom Res C, 2015, 56: 109–118
101 Du L, Su G. Adaptive inverse synthetic aperture radar imaging for nonuniformly moving targets. IEEE Geosci Remote Sens Lett, 2005, 2: 247–249
102 Xing M, Wu R, Li Y, et al. New ISAR imaging algorithm based on modified Wigner-Ville distribution. IET Radar Sonar Navig, 2009, 3: 70–80
103 Tao R, Zhang N, Wang Y. Analysing and compensating the effects of range and Doppler frequency migrations in linear frequency modulation pulse compression radar. IET Radar Sonar Navig, 2011, 5: 12–22
104 Thayaparan T, Brinkman W, Lampropoulos G. Inverse synthetic aperture radar image focusing using fast adaptive joint time-frequency and three-dimensional motion detection on experimental radar data. IET Signal Process, 2010, 4: 382
105 Brinkman W, Thayaparan T. Focusing inverse synthetic aperture radar images with higher-order motion error using the adaptive joint-time-frequency algorithm optimised with the genetic algorithm and the particle swarm optimisation algorithm – comparison and results. IET Signal Process, 2010, 4: 329–342
106 Kang B S, Bae J H, Lee S J, et al. ISAR rotational motion compensation algorithm using polynomial phase transform. Microw Opt Technol Lett, 2016, 58: 1551–1557
107 Kang B S, Kang M S, Choi I O, et al. Efficient autofocus chain for ISAR imaging of non-uniformly rotating target. IEEE Senss J, 2017, 17: 5466–5478
108 Liu L, Qi M S, Zhou F. A novel non-uniform rotational motion estimation and compensation method for maneuvering targets ISAR imaging utilizing particle swarm optimization. IEEE Senss J, 2018, 18: 299–309
109 Ye C M, Xu J, Peng Y N, et al. Improved Doppler centroid tracking for ISAR based on target extraction. In: Proceedings of IEEE Radar Conference, 2008
110 Pellizzari C J, Bos J, Spencer M F, et al. Performance characterization of phase gradient autofocus for inverse synthetic aperture LADAR. In: Proceedings of IEEE Aerospace Conference, Place, 2014
111 Zhou S, Xing M D, Xia X G, et al. An azimuth-dependent phase gradient autofocus (APGA) algorithm for airborne/stationary BiSAR imagery. IEEE Geosci Remote Sens Lett, 2013, 10: 1290–1294
112 Wang J F, Kasilingam D, Liu X Z, et al. ISAR minimum-entropy phase adjustment. In: Proceedings of IEEE Radar Conference, 2004. 197–200
113 Cao P, Xing M D, Sun G C, et al. Minimum entropy via subspace for ISAR autofocus. IEEE Geosci Remote Sens Lett, 2010, 7: 205–209
114 Cai J J, Xu J, Wang G, et al. An effective ISAR autofocus algorithm based on single eigenvector. In: Proceedings of IEEE International Radar Conference, Guangzhou, 2016
115 Lee S H, Bae J H, Kang M S, et al. Efficient ISAR autofocus technique using eigenimages. IEEE J Sel Top Appl Earth Observations Remote Sens, 2017, 10: 605–616
116 Xu J, Cai J J, Sun Y H, et al. Efficient ISAR phase autofocus based on eigenvalue decomposition. IEEE Geosci Remote Sens Lett, 2017, 14: 2195–2199
117 Liu H W, Chen F, Du L, et al. Robust radar automatic target recognition algorithm based on HRRP signature. Front Electr Electron Eng China, 2012, 7: 49–55
118 Jing C, Tao Z, Mian P, et al. Radar HRRP recognition based on discriminant deep autoencoders with small training data size. Electron Lett, 2016, 52: 1725–1727
119 Feng B, Chen B, Liu H W. Radar HRRP target recognition with deep networks. Pattern Recogn, 2017, 61: 379–393
120 Duan P P, Li H. The radar target recognition research based on improved neural network algorithm. In: Proceedings of International Conference on Intelligent Systems Design and Engineering Applications (ISDEA), 2014. 1074–1077
121 Penacaballero C, Cantu E, Rodriguez J. Automatic target recognition of aircraft using inverse synthetic aperture radar. 2017. ArXiv:1711.04901

122 Jiang Y, Xu J, Peng S B, et al. Identification-while-scanning of a multi-aircraft formation based on sparse recovery for narrowband radar. Sensors, 2016, 16: 1972
123 Pan M, Jiang J, Kong Q P, et al. Radar HRRP target recognition based on t-SNE segmentation and discriminant deep belief network. IEEE Geosci Remote Sens Lett, 2017, 14: 1609–1613
124 Dai W L, Zhang G, Zhang Y. HRRP classification based on multi-scale fusion sparsity preserving projections. Electron Lett, 2017, 53: 748–750
125 Du L, Wang P H, Liu H W, et al. Bayesian spatiotemporal multitask learning for radar HRRP target recognition. IEEE Trans Signal Process, 2011, 59: 3182–3196
126 Zhou D Y, Shen X F, Yang W L. Radar target recognition based on fuzzy optimal transformation using high-resolution range profile. Pattern Recogn Lett, 2013, 34: 256–264
127 Du L, Liu H W, Bao Z, et al. Radar automatic target recognition using complex high-resolution range profiles. IET Radar Sonar Navig, 2007, 1: 18–26
128 Du L, Liu H W, Bao Z. Radar HRRP statistical recognition: parametric model and model selection. IEEE Trans Signal Process, 2008, 56: 1931–1944
129 Schölkopf B, Smola A J, Müller K R. Nonlinear component analysis as a kernel eigenvalue problem. Neural Comput, 1998, 10: 1299–1319
130 Kim K T, Seo D K, Kim H T. Efficient radar target recognition using the MUSIC algorithm and invariant features. IEEE Trans Antennas Propagat, 2002, 50: 325–337
131 Aldhubaib F, Shuley N V. Radar target recognition based on modified characteristic polarization states. IEEE Trans Aerosp Electron Syst, 2010, 46: 1921–1933
132 Wang F Y, Guo R J, Huang Y H. Radar target recognition based on some invariant properties of the polarization scattering matrix. In: Proceedings of IEEE International Radar Conference, Place, 2011. 626–629
133 Li X, Lin L S, Shao X H, et al. A target polarization recognition method for radar echoes. In: Proceedings of International Conference on Microwave and Millimeter Wave Technology, Place, 2010. 1644–1647
134 Long T, Mao E K, He P K. Analysis and processing of modulated frequency stepped radar signal. Acta Electron Sin, 1998, 12: 84–88